Solvent Effects on the Barrier to C−N Bond Rotation in *N*,*N*-Dimethylaminoacrylonitrile

Paul R. Rablen,* Deborah A. Miller, Valerie R. Bullock, Peter H. Hutchinson, and Jessica A. Gorman

Contribution from the Department of Chemistry, Swarthmore College, 500 College Ave., Swarthmore, Pennsylvania 19081-1397

Received July 1, 1998

Abstract: The barrier to rotation about the conjugated C−N bond of *N*,*N*-dimethylaminoacrylonitrile (DMAAN) was determined by dynamic NMR spectroscopy in the solvents methylcyclohexane, dibutyl ether, toluene, dichloromethane, chloroform, acetone, acetonitrile, nitromethane, methanol, and water. The barrier was found to increase with solvent polarity, as is the case for amides. In striking contrast to amides, however, the barrier was found *not* to depend on solvent hydrogen bond donor ability. For aprotic solvents, the variation of the DMAAN barrier with solvent correlated closely with the solvent dependence previously observed for the rotational barriers of dimethylformamide (DMF) and dimethylacetamide (DMA). Comparison of the solvent dependence of the barriers in these two compounds was used to estimate the gas-phase barrier in DMAAN at 9.3 kcal/mol. High-level ab initio calculations yielded good agreement with the gas-phase barrier extrapolated from the experimental data. For aprotic solvents, the solvent effects were linearly related to Brownstein's empirical solvent polarity parameter *S*. For a subset of solvents that were nonaromatic and non-chlorinated as well as aprotic, the barrier correlated closely with the Onsager dielectric function, $(\epsilon - 1)/(2\epsilon + 1)$. The estimate for the gas-phase barrier of DMAAN obtained from this correlation agreed closely with that derived earlier on the basis of the relationship with the DMA barriers. A calculated difference density plot showed that little electronic reorganization occurs at the nitrile functional group of DMAAN during rotation about the C−N bond.

Introduction

Conformational isomerization processes, such as rotation about the C−N bonds of amides, have long held great interest for organic chemists.[1−4] Some of this interest derives from the clues about electronic structure provided by the corresponding potential energy barriers.[4,5] For instance, in the case of amides, the large C−N rotational barrier provides clear experimental evidence for an interaction between the nitrogen lone pair and the carbonyl group. Another source of motivation arises from biochemical applications, such as the important role that peptide bond isomerization in proline residues can play in limiting the rate of protein folding[6] and the observation of rotamase enzymes that catalyze this isomerization.[6,7] Solvent effects constitute a second general topic of continuing relevance.[8] Much interest in solvent effects is motivated by the fact that while most reactions are carried out in solution, many common ideas about reactivity implicitly pertain to isolated molecules and thus the gas phase. Furthermore, molecular orbital calculations, which are ever more widely used, yield predictions that are strictly valid only for the gas phase. Application of such calculations to reactions and structures in solution requires at least a semiquantitative understanding of the solvent's influence, if not in fact the ability to calculate this influence quantitatively. The solution environment often plays a critical role in biological systems, making the issue of solvent effects and their calculation especially germane in the current research environment.[9,10]

Many computational schemes for predicting solvation energies are currently under development.[10−22] However, these models require calibration and testing against experimental data. Conformational isomerizations represent some of the simplest

(1) Orville-Thomas, W. J. *Internal Rotation in Molecules*; John Wiley & Sons: New York, 1974.

(2) (a) Stewart, W. E.; Siddall, T. H., III *Chem. Rev.* **1970**, *70*, 517−551 and references therein. (b) Drakenberg, T.; Dahlqvist, K. J.; Forsen, S. *J. Phys. Chem.* **1972**, *76*, 2178−2183.

(3) (a) Cox, C.; Young, V. G., Jr.; Lectka, T. *J. Am. Chem. Soc.* **1997**, *119*, 2307−2308. (b) Cox, C.; Ferraris, D.; Murthy, N. N.; Lectka, T. *J. Am. Chem. Soc.* **1996**, *118*, 5332−5333.

(4) Kessler, H. *Angew. Chem., Int. Ed. Engl.* **1970**, *9*, 219−235.

(5) For example: Neugebauer Crawford, S. M.; Taha, A. N.; True, N. S.; LeMaster, C. B. *J. Phys. Chem. A* **1997**, *101*, 4699−4706.

(6) (a) Schmid, F. X. In *Protein Folding*; Creighton, T. E., Ed.; W. H. Freeman: New York, 1992; pp 197−241, see also other chapters in this book. (b) Schmid, F. X.; Mayr, L. M.; Mücke, M.; Schönbrunner, E. R. *Adv. Protein Chem.* **1993**, *44*, 25−66. (c) Eberhardt, E. S.; Loh, S. N.; Hinck, A. P.; Raines, R. T. *J. Am. Chem. Soc.* **1992**, *114*, 5437−5439 and references therein. (d) Stein, R. L. *Adv. Protein Chem.* **1993**, *44*, 1−24.

(7) (a) Schreiber, S. L. *Science* **1991**, *251*, 283−287. (b) Gething, M.-J.; Sambrook, J. *Nature* **1992**, *355*, 33−45. (c) Fischer, G.; Schmid, F. X. *Biochemistry* **1990**, *29*, 2205−2212.

(8) Reichardt, C. *Solvents and Solvent Effects in Organic Chemistry, 2nd ed.*; VCH Publishers: Germany, 1988.

(9) McCammon, A.; Harvey, S. C. *Dynamics of Proteins and Nucleic Acids*; Cambridge University Press: Cambridge, 1987.

(10) (a) Gould, I. R.; Cornell, W. D.; Hillier, I. H. *J. Am. Chem. Soc.* **1994**, *116*, 9250−9256. (b) Adamo, C.; Dillet, V.; Barone, V. *Chem. Phys. Lett.* **1996**, *263*, 113−118. (c) Pierce, A. C.; Jorgensen, W. L. *Angew. Chem., Int. Ed. Engl.* **1997**, *36*, 1466−1469. (d) Rao, B. G.; Kim, E. E.; Murcko, M. A. *J. Comput.-Aid. Mol. Des.* **1996**, *10*, 23. (e) Yang, B.; Wright, J.; Eldefrawi, M. E.; Pou, S.; MacKerell, A. D., Jr. *J. Am. Chem. Soc.* **1994**, *116*, 8722−8732. (f) Zheng, Y.-J.; Ornstein, R. L. *J. Am. Chem. Soc.* **1997**, *119*, 648−655. (g) Urban, J. J.; Cronin, C. W.; Roberts, R. R.; Famini, G. R. *J. Am. Chem. Soc.* **1997**, *119*, 12292−12299.

(11) For reviews of continuum solvation models, see: (a) Tomasi, J.; Persico, M. *Chem. Rev.* **1994**, *94*, 2027−2094. (b) Cramer, C. J.; Truhlar, D. G. *Rev. Comput. Chem.* **1990**, *6*, 1−72.

10.1021/ja982304f CCC: $18.00
Published on Web 12/22/1998

and structurally most well-defined reactions known, and consequently are particularly well suited to this sort of validation. In principle, both conformational equilibria and rates of conformational change can be studied. A number of studies of the solvent dependence of conformational equilibria have been published,[8,10g,13,23,24] although there is still a need for additional systematic experimental data concerning a wide variety of systems in a broad selection of solvents. However, relatively few systematic studies of solvent effects on conformational isomerization rates have been performed.[2,3,8,24−28] The rate constants yield information about the relative solvent stabilization of the equilibrium structure (minimum) and the transition state for an isomerization reaction, and thus allow an examination of how well various models reproduce the relative solvation energies of the equilibrium and transition state structures.

One type of conformational isomerization process for which detailed kinetic studies have been carried out previously is rotation about the C−N bond of amides. This process is known to be retarded by polar solvents, and particularly detailed data are available for *N*,*N*-dimethylformamide (DMF) (**1a**) and *N*,*N*-dimethylacetamide (DMA) (**1b**).[2,25,29] Additionally, computational modeling has been carried out on both of these systems.[25,30,31] Each of these amides has two possible transition states for rotation, since the nitrogen becomes pyramidal in the transition state, and the lone pair can point in a direction either syn or anti to the carbonyl oxygen. These transition states are shown and labeled in Scheme 1. The transition state structure of DMA having the lone pair anti to the carbonyl (DMA TS #1, **2b**) is favored in the gas phase and in aprotic solvents, although calculations suggest that the "syn" structure (**3b**) might be competitive or even preferred in aqueous solution.[30] With DMF, on the other hand, the "syn" structure (DMF TS #2, **3a**) is predicted by calculation to be favored under all circumstances, although the "anti" structure (**2a**) is only slightly higher in energy in the gas phase and in nonpolar solvents. The gas-phase barriers have been measured experimentally by NMR spectroscopy,[32] and the agreement with high-level ab initio predictions (e.g., with Pople's G-2 procedure[33]) is within 0.5 kcal/mol.[25]

Scheme 1

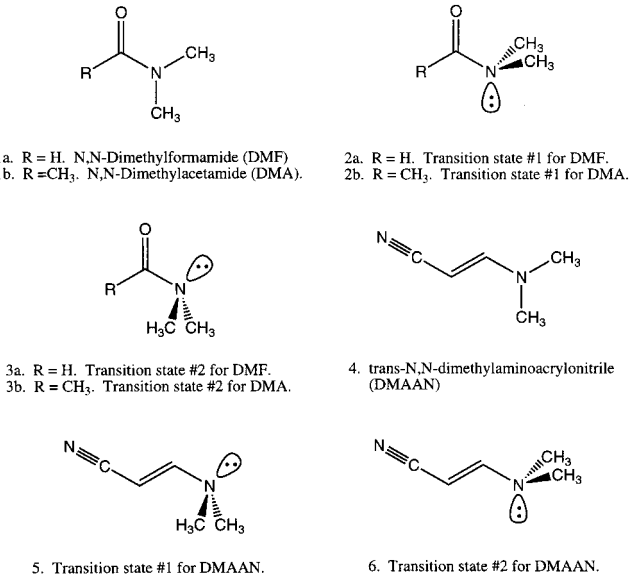

The transition states for DMF and DMA are predicted to have lower dipole moments than the equilibrium structures, although the difference is more pronounced for the case of DMA, which prefers the "anti" transition state. Simple electrostatic considerations then predict that a more polar environment should raise the barrier to bond rotation, and that the effect should be larger for DMA than for DMF. Experimental measurements have confirmed this prediction.[2,25] Moreover, the magnitude of the solvent effect agrees very well with the predictions of a polarizable continuum reaction field model, at least for certain "well-behaved" aprotic solvents that lack second-row elements and aromatic rings.[25] According to this model, the magnitude of the solvent effect has a very nearly linear dependence on the Onsager dielectric function, defined as $(\epsilon - 1)/(2\epsilon + 1)$, where ϵ is the dielectric constant. Others have attributed the observed solvent effects to solvent internal pressure and to the greater volume requirements of the transition state structures in comparison to the equilibrium structure.[29]

The protic solvents methanol and water increase the observed barriers to rotation in DMA and DMF substantially beyond what

(12) (a) Mennucci, B.; Tomasi, J. *J. Chem. Phys.* **1997**, *106*, 5151−5158 and references therein. (b) Miertus, S.; Scrocco, E.; Tomasi, J. *Chem. Phys.* **1981**, *55*, 117−129. (c) Tomasi, J.; Bonaccorsi, R.; Cammi, R.; Valle, F. O. J. *J. Mol. Struct.* **1991**, *234*, 401.

(13) Foresman, J.; Keith, T. A.; Wiberg, K. B.; Snoonian, J.; Frisch, M. *J. Phys. Chem.* **1996**, *100*, 16098−16104.

(14) Kollman, P. A. *Chem. Rev.* **1993**, *93*, 2395−2417.

(15) (a) Gao, J.; Freindorf, M. *J. Phys. Chem. A* **1997**, *101*, 3182−3188. (b) Gao, J. L. *Acc. Chem. Res.* **1996**, *29*, 298−305. (c) Gao, J.; Alhambra, C. *J. Am. Chem. Soc.* **1997**, *119*, 2962−2963.

(16) Truong, T. N.; Stefanovich, E. V. *J. Phys. Chem.* **1995**, *99*, 14700−14706. Truong, T. N.; Truong, T.-T. T.; Stefanovich, E. V. *J. Phys. Chem.* **1997**, *107*, 11881−1889.

(17) Marten, B.; Kim, K.; Cortis, C.; Friesner, R. A.; Murphy, R. B.; Ringnalda, M. N.; Sitkoff, D.; Honig, B. *J. Phys. Chem.* **1996**, *100*, 11775−11788.

(18) Chen, W.; Gordon, M. S. *J. Chem. Phys.* **1996**, *105*, 11081−11090.

(19) Bader, J. S.; Cortis, C. M.; Berne, B. J. *J. Chem. Phys.* **1997**, *106*, 2372−2387.

(20) Giesen, D. J.; Gu, M. Z.; Cramer, C. J.; Truhlar, D. G. *J. Org. Chem.* **1996**, *61*, 8720−8721. Chambers, C. C.; Hawkins, G. D.; Cramer, C. J.; Truhlar, D. G. *J. Phys. Chem.* **1996**, *100*, 16385−16398.

(21) Hummer, G.; Pratt, L. R.; García, A. E. *J. Am. Chem. Soc.* **1997**, *119*, 8523−8527.

(22) Still, W. C.; Tempczyk, A.; Hawley, R. C.; Hendrickson, T. *J. Am. Chem. Soc.* **1990**, *112*, 6127−6129.

(23) (a) Perrin, C. L.; Fabian, M. A.; Rivero, I. A. *J. Am. Chem. Soc.* **1998**, *120*, 1044−1047. (b) Nagy, P. I.; Takács-Novák, K. *J. Am. Chem. Soc.* **1997**, *119*, 4999−5006. (c) Wong, M. W.; Wiberg, K. B.; Frisch, M. J. *J. Am. Chem. Soc.* **1992**, *114*, 1645−1652. (d) Wiberg, K. B.; Wong, M. W. *J. Am. Chem. Soc.* **1993**, *115*, 1078−1084. (e) Wiberg, K. B.; Marquez, M. M. *J. Am. Chem. Soc.* **1994**, *116*, 2197−2198. (f) Jorgensen, W. L.; Morales de Tirado, P. I.; Severance, D. L. *J. Am. Chem. Soc.* **1994**, *116*, 2199−2200. (g) Wiberg, K. B.; Keith, T. A.; Frisch, M. J.; Murcko, M. *J. Phys. Chem.* **1995**, *99*, 9072−9079.

(24) Chiara, J. L.; Gómez-Sánchez, A.; Bellanato, J. *J. Chem. Soc., Perkin Trans. 2* **1992**, 787−798.

(25) Wiberg, K. B.; Rablen, P. R.; Rush, D. J.; Keith, T. A. *J. Am. Chem. Soc.* **1995**, *117*, 4261−4270.

(26) Craw, J. S.; Guest, J. M.; Cooper, M. D.; Burton, N. A.; Hillier, I. H. *J. Phys. Chem.* **1996**, *100*, 6304−6309.

(27) Pappalardo, R. R.; Marcos, E. S.; Ruiz-López, M. F.; Rinaldi, D.; Rivail, J.-L. *J. Am. Chem. Soc.* **1993**, *115*, 3722−3730.

(28) Filleux-Blanchard, M. L.; Clesse, F.; Bignebat, J.; Martin, G. J. *Tetrahedron Lett.* **1969**, *12*, 981−984.

(29) Suarez, C.; LeMaster, C. B.; LeMaster, C. L.; Tafazzoli, M.; True, N. S. *J. Phys. Chem.* **1990**, *94*, 6679−6683.

(30) Duffy, E. M.; Severance, D. L.; Jorgensen, W. L. *J. Am. Chem. Soc.* **1992**, *114*, 7535−7542.

(31) Gao, J. *J. Am. Chem. Soc.* **1993**, *115*, 2930−2935. Gao, J. *Proc. Indian Acad. Sci.* **1994**, *106*, 507.

(32) (a) Ross, B. D.; True, N. S. *J. Am. Chem. Soc.* **1984**, *106*, 2451−2452. Cf. LeMaster, C. B.; True, N. S. *J. Phys. Chem.* **1989**, *93*, 1307−1311. (b) Ross, B. D.; True, N. S.; Matson, G. B. *J. Phys. Chem.* **1984**, *88*, 2675−2678. (c) Feigel, M. *J. Chem. Soc. Chem. Commun.* **1980**, 456. (d) Feigel, M. *J. Phys. Chem.* **1983**, *87*, 3054−3058. The $\Delta G^{\ddagger}$ values reported in (c) and (d) were based on a transmission coefficient of 1.0, and were recalculated by using 0.5 to be consistent with the values given in (a) and (b) and the values reported in the current work.

(33) (a) Curtiss, L. A.; Raghavachari, K.; Trucks, G. W.; Pople, J. A. *J. Chem. Phys.* **1991**, *94*, 7221−7230. (b) Curtiss, L. A.; Carpenter, J. E.; Raghavachari, K.; Pople, J. A. *J. Chem. Phys.* **1992**, *96*, 9030−9034.

Table 1. Ab Initio Calculated Dipole Moments and Barriers to Rotation about the Conjugated C−N Bond in *N*,*N*-Dimethylaminoacrylonitrile[a,b]

	HF/6-31G*		MP2/6-31G*		MP2[c]		MP3[c]	QCISD[d]
species	$\Delta H_0°$	μ	$\Delta H_0°$	μ	$\Delta H_0°$	μ	$\Delta H_0°$	$\Delta H_0°$
ES	0.0	6.89	0.0	6.48	0.0	6.66	0.0	0.0
TS1	11.4	4.75	12.0	4.15	12.3	4.22	11.1	11.2
TS2	7.7	4.98	8.3	4.43	8.4	4.48	7.4	7.5

[a] All energies listed are gas-phase enthalpies at 0 K and include ZPE calculated at the HF/6-31G* level and scaled by 0.8934. [b] Energies in kcal/mol; dipole moments in Debye units. [c] Basis set 6-311++G**; MP2/6-31G* optimized geometry. [d] Basis set 6-311+G**; MP2/6-31G* optimized geometry.

would be predicted on the basis of the dielectric constants alone. This effect has been attributed to hydrogen-bond donation by the solvent, and is in accord with the calculated effect of adding a single water molecule to the equilibrium and transition state structures of DMF. As might be expected, the hydrogen-bonding interaction between a single water molecule and the carbonyl oxygen of DMF is significantly stronger for the equilibrium structure than for the transition state structure, leading to an increased barrier height.[25]

We were interested in examining another case of rotation about a conjugated C−N bond, to see whether a similar pattern would emerge in the solvent effects themselves and in the abilities of various solvation models to reproduce the experimental data. We have chosen for study *trans*-*N*,*N*-dimethylaminoacrylonitrile (DMAAN, **4**), which resembles a vinylogous amide. We were particularly interested to see how the barriers to C−N bond rotation in DMAAN in a variety of solvents would compare to the corresponding data for DMA and DMF, and to determine whether a polarizable continuum model would again prove successful for "well-behaved" solvents. This paper presents experimental measurements along with an empirical analysis of the results and a comparison to the predictions of gas-phase ab initio calculations. The following paper in this issue examines how well the experimental results are reproduced by two solvation models, one of which uses explicit representations of solvent molecules and the other of which employs a continuum description.

Results

Gas-Phase Calculated Barriers. The equilirium structure of DMAAN has a nearly planar geometry that allows conjugation between the lone pair electrons on the amino group and the vinylogous nitrile functionality. Although the minimum energy structure has C_1 symmetry, the deviations from C_s symmetry (planarity) are small, and are dominated by a slight degree of pyramidalization at the amino nitrogen. Both the nearly planar geometry (sp^2 hybridization) at the amino nitrogen and the large barrier to rotation about the C−N bond result from donation by the nitrogen lone pair into the rest of the π system.

As with DMF and DMA, C−N bond rotation in DMAAN can take place through either of two transition states which differ in the direction of pyramidalization at the amino nitrogen, and which are shown in Scheme 1 as structures **5** and **6**. As can be seen from the data in Table 1, at a variety of levels of ab initio theory ranging from HF/6-31G* to MP3/6-311++G**//MP2/6-31G* and QCISD/6-311+G**//MP2/6-31G* TS #2 (**6**) is consistently lower in energy than TS #1 (**5**) by 3.7 to 3.9 kcal/mol. The degree of consistency in the energy difference between the transition states lends confidence to the prediction that, at least in the gas phase, TS #2 is by far the dominant transition state structure. The magnitude of the predicted barrier ranges from 7.4 to 8.4 kcal/mol, corresponding to roughly half the value for DMF (19.3) or DMA (15.3). Both transition state structures are calculated to have dipole moments approximately 30% smaller than that of the equilibrium structure, as shown in Table 1, again parallel to the observations for DMF and DMA. The greater polarity of the nearly planar equilibrium conformation can be attributed to the dipolar resonance contributor that is not possible in the rotated conformations.

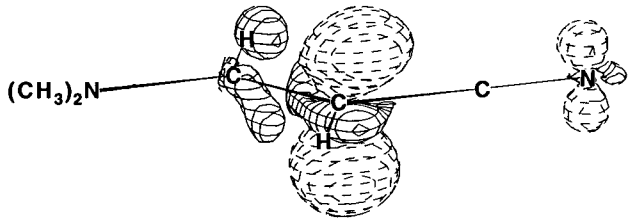

Figure 1. MP2/6-311++G**(6D)//MP2/6-31G* calculated difference densities for rotation about the conjugated C−N bond of DMAAN. The surfaces shown represent the $\pm 2.5 \times 10^{-3}$ electron/Bohr^3 contours. The solid lines represent positive electron density and the dashed lines represent negative electron density. The difference density is defined here as the electron density for the transition state structure (TS#2) minus that for the equilibrium structure (ES).

Difference Density Calculations. A difference density was computed to quantify and visualize the charge redistribution that occurs during rotation about the C−N bond of DMAAN. The calculation was carried out at the MP2/6-311++G**//MP2/6-31G* level of theory with use of methodology previously developed for studying bond rotation in amides and thioamides,[34] and the results are illustrated graphically in Figure 1. The procedure is described in somewhat more detail in the Experimental Section, but in essence the charge density for the equilibrium structure is subtracted from that for the transition state to reveal what changes occur as a result of bond rotation. In addition, the charge density associated with the dimethylamino group has been removed so that changes in the remainder of the molecule can be seen more clearly. The extent of electronic reorganization was further quantified by direct integration of the domains visible in Figure 1, yielding the following results: cyano nitrogen, $-0.016\ \pi$, $+0.004\ \sigma$; vinylic carbon, $-0.074\ \pi$, $+0.029\ \sigma$ (all numbers in electron charge units). It is evident that very little charge reorganization occurs at the cyano group. This observation bears on the topic of hydrogen bonding to DMAAN in protic solvents, which is addressed below in the context of the rotational barriers in methanol and water.

Thermodynamic Corrections. The energy differences reported in Table 1 include zero-point energy (ZPE) corrections based on the HF/6-31G* calculated vibrational frequencies scaled by the conventional factor of 0.8934,[33] and thus represent enthalpies at absolute zero. Reliable comparison to experimental measurements requires the further inclusion of thermodynamic corrections to yield calculated free energies at the experimentally relevant temperatures. In the case where all modes are harmonic, or at least close to harmonic, such corrections are routine.[35] However, vibrational modes that are not well-described in this manner, such as the rotation of methyl groups or the inversion motion at tricoordinate nitrogen, require a more involved treatment. In the cases of DMF and DMA, these corrections have been worked out in detail.[25]

(34) Wiberg, K. B.; Rablen, P. R. *J. Am. Chem. Soc.* **1995**, *117*, 2201−2209.

(35) Janz, G. J. *Thermodynamic Properties of Organic Compounds: Estimation Methods, Principles and Practice*, revised edition; Academic Press: New York, 1967.

Table 2. Thermodynamic Corrections at 273 K (kcal/mol)

	$G° - G_0°$ (273 K)					
species	trans.	rot.	vibr.	N−inv.[a]	Me-rot[a]	total
ES	−9.33	−6.71	−1.35	−0.50	−0.99	−18.88
TS1	−9.33	−6.70	−0.90	0.00	−0.52	−17.45
TS2	−9.33	−6.71	−0.84	0.00	−0.52	−17.40
TS1-ES	0.00	+0.01	+0.45	+0.50	+0.47	+1.43
TS2-ES	0.00	0.00	+0.51	+0.50	+0.47	+1.48

[a] Taken from: Wiberg, K. B.; Rablen, P. R.; Rush, D. J.; Keith, T. A. *J. Am. Chem. Soc.* **1995**, *117*, 4261−4270.

Nonetheless, deviations from predictions that use only harmonic approximations are relatively small, and the contributions to solvent effects are smaller still. As our current interest lies primarily with solvent effects, we have not attempted to carry out a rigorously correct series of thermodynamic corrections, and have provided instead the approximate corrections appearing in Table 2. We have used strictly harmonic corrections for all but the three lowest-frequency modes of the equilibrium structure, and all but the imaginary frequency and the two lowest frequency real modes for the transition state structures. The modes that were ignored in the harmonic treatment are associated with the two methyl rotations and inversion at nitrogen. Under the assumption that these modes closely resemble the corresponding ones in DMF, we have taken the thermodynamic corrections reported by Wiberg et al. for the methyl rotation and nitrogen inversion modes of DMF and applied them to DMAAN.[25,36] It is worthy of note that improper treatment of these unusual modes will only affect the calculated barriers to rotation if the degree of error is different in the transition states than in the equilibrium structure, and that the consequences for the calculated solvent effects should be entirely negligible in any case. Including the appropriate thermodynamic corrections, the ab initio estimates of the free energy barrier to C−N bond rotation in DMAAN at 273 K range from 8.9 (MP3) to 9.9 (MP2) kcal/mol. The single most reliable value is probably the 9.0 kcal/mol derived from the QCISD calculation.

Experimental Determination of Barriers to C−N Bond Rotation in DMAAN. Table 3 lists barriers to rotation about the conjugated C−N bond of DMAAN in a variety of solvents, determined via dynamic NMR spectroscopy at temperatures in the vicinity of 273 K. The barriers were derived from observed rate constants under the assumption of statistical kinetics (RRKM theory). Most determinations of the rate of exchange between the methyl groups were performed by line shape fitting,[4,37−39] but some selective inversion−recovery (magnetization transfer) experiments[40−42] were carried out as well. Although applicable to somewhat different rate constant regimes, and therefore somewhat different temperatures, the two methods yielded results that were in excellent agreement with each other. The free energy barriers determined in chloroform (12.63 kcal/mol) and in dichloromethane (12.71 kcal/mol) also agree quite closely with results reported previously in carbon tetrachloride (12.9 kcal/mol).[43]

Table 3. Experimentally Determined Barriers to Rotation about the Conjugated C−N Bond in *N,N*-Dimethylaminoacrylonitrile (kcal/mol)

solvent	ϵ[a]	S[b]	$\Delta G^{‡}(273)$[c]	$\Delta H^{‡}$	$\Delta S^{‡}$
gas phase	1.0	−0.556	9.3 ± 0.5[d]		
methylcyclohexane-d_{14}	2.0	−0.324	11.0 ± 0.2		
toluene-d_8	2.4	−0.237	12.05	12.9	+3.0
dibutyl ether-d_{18}	3.1	−0.286	11.54	12.9	+5.0
chloroform-d	4.8	−0.200	12.63	12.8	+0.7
dichloromethane-d_2	8.9	−0.189	12.71	12.6	−0.5
acetone-d_6	20.6	−0.175	12.80	13.4	+2.3
methanol-d_4	32.7	+0.050	12.96	12.5	−1.7
acetonitrile-d_3	35.9	−0.104	13.34	13.8	+1.8
nitromethane-d_3	35.9	−0.134	13.13	12.7	−1.7
water-d_2	78.0		≤13.0		

[a] Dielectric constant. Source: Reichardt, C. *Solvents and Solvent Effects in Organic Chemistry*, 2nd ed.; VCH: New York, 1990. [b] Empirical solvent polarity parameter *S*: Brownstein, S. *Can. J. Chem.* **1960**, *38*, 1590. [c] Free energy of activation for the bond rotation process at 273 K. [d] Gas-phase barrier extrapolated from available experimental data on the basis of correlation with previously determined DMA data and with the Onsager dielectric function, $(\epsilon - 1)/(2\epsilon + 1)$.

Rate constants were determined at a number of temperatures whenever possible, so that the temperature dependence of the rates could be obtained. This temperature dependence is required to make proper comparisons between different systems. The full set of available rate constants in a given solvent was used to interpolate or extrapolate the rate of exchange at 273 K, from which $\Delta G^{‡}$ was calculated. This approach ensures that comparisons between different solvents are made under a single, consistent set of conditions representing a single temperature. The individual experimentally determined rate constants are provided in the Supporting Information. The transmission coefficient in the Eyring equation was set to 0.5, as is appropriate for a symmetrical exchange process, and is consistent with earlier practice for the cases of DMA and DMF.[25,32] Transition state enthalpies and entropies are also provided in Table 3, although they are subject to much greater uncertainty than the $\Delta G^{‡}(298)$ values, and the latter are used for all subsequent analysis. The consistently small entropies are, however, consistent with previous studies of bond rotation in amides.[2,32]

Definitive experiments were not possible at the two extreme ends of polarity on the solvent scale. In methylcyclohexane, the two methyl peaks of DMAAN begin to de-coalesce as the temperature drops below 275 K. However, once the temperature drops below 235 K, the solubility of DMAAN decreases to the point where significant precipitation occurs even in solutions of very low concentration, and NMR spectroscopy becomes impossible. At the opposite end of the scale, water freezes before the rate of methyl group exchange becomes sufficiently slow that two separate peaks appear in the spectrum. However, both these cases are of considerable importance, and partial information is available via the broadened spectra taken in the relatively

(36) Since there is no way to correlate the two different transition states of DMF with those of DMAAN, we have simply used the average of the values reported for the two DMF transition states. The differences in the thermodynamic corrections for methyl rotation and nitrogen inversion between the two DMF transition states are extremely small (less than 0.05 kcal/mol).

(37) Sandström, J. *Dynamic NMR Spectroscopy*; Academic Press: New York, 1982.

(38) Kaplan, J. I.; Fraenkel, G. *NMR of Chemically Exchanging Systems*; Academic Press: New York, 1980.

(39) Gutowsky, H. S.; Holm, C. H. *J. Chem. Phys.* **1956**, *25*, 1228−1234.

(40) (a) Forsén, S.; Hoffman, R. A. *Acta Chem. Scand.* **1963**, *17*, 1787. (b) Dahlquist, F. W.; Longmuir, K. J.; DuVernet, R. B. *J. Magn. Reson.* **1975**, *17*, 406.

(41) (a) Mann, B. E. *J. Magn. Reson.* **1976**, *21*, 17. (b) Alger, J. R.; Prestegard, J. H. *J. Magn. Reson.* **1977**, *27*, 137. (c) Led, J. J.; Gesmar, H. *J. Magn. Reson.* **1982**, *49*, 444. (d) Gesmar, H.; Led, J. J. *J. Magn. Reson.* **1986**, *68*, 95. (e) Grassi, M.; Mann, B. E.; Pickup, B. T.; Spencer, C. M. *J. Magn. Reson.* **1986**, *69*, 92. (f) Engler, R. E.; Johnston, E. R.; Wade, C. G. *J. Magn. Reson.* **1988**, *77*, 377.

(42) Perrin, C. L.; Thoburn, J. D.; Kresge, A. J. *J. Am. Chem. Soc.* **1992**, *114*, 8800−8807.

(43) Hobson, R. F.; Reeves, L. W. *J. Phys. Chem.* **1973**, *77*, 419−422. This study does not report rate constants (only energy barriers), and does not specify whether a transmission coefficient of 1.0 or 0.5 was used, and so the value reported for the barrier to DMAAN C−N bond rotation in carbon tetrachloride cannot reliably be compared to the present results in an exact manner.

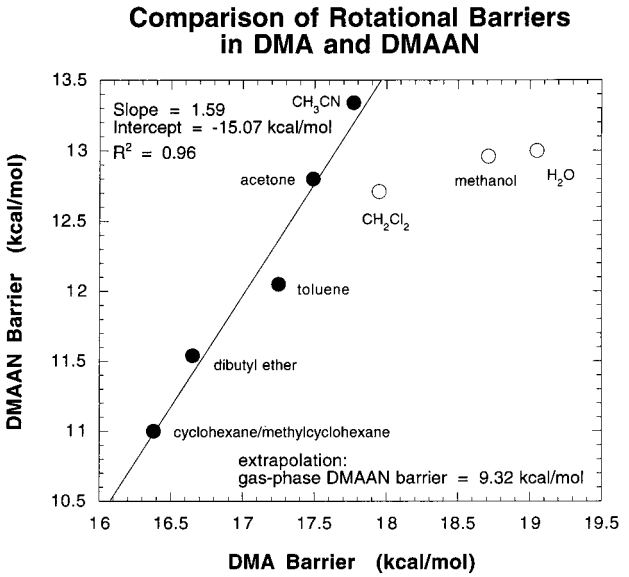

Figure 2. Relationship between the barrier to C−N bond rotation in DMA and DMAAN as a function of solvent. Best fit line: DMAAN = 1.59∗DMA + 15.07; r^2 = 0.96 (energies in kcal/mol). The data points represented by open circles were excluded from the fit.

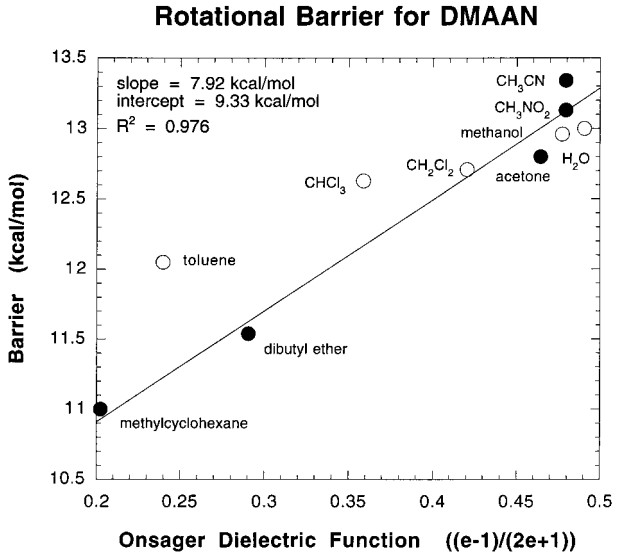

Figure 3. Relationship between the experimental barrier to C−N bond rotation in DMAAN and the Onsager dielectric function, $(\epsilon - 1)/(2\epsilon + 1)$, of the solvent. Best fit line: barrier (kcal/mol) = 9.33∗$(\epsilon - 1)/(2\epsilon + 1)$ + 7.92; r^2 = 0.98. The data points represented by open circles were excluded from the fit.

fast exchange regime. Consequently, estimates of the barriers in these solvents have been included in Table 3. With D_2O, the available data permit the estimation of a lower limit on the exchange rate, and thus an upper limit on the barrier. In the case of methylcyclohexane, the degree of separation of the peaks at 238 K is sufficient to permit the actual determination of a rate constant, although with ±25% uncertainty. Nonetheless, even the approximate rate constant provides an estimate of the barrier with an uncertainty of ±0.1 kcal/mol at 238 K. Assuming as in other cases the contribution of $\Delta S^{\ddagger}$ is small, the value of 11.0 ± 0.2 kcal/mol is taken as the value of $\Delta G^{\ddagger}$ at 273 K, with the additional uncertainty listed representing the extrapolation from 238 to 273 K.

Experimental Estimation of the Gas-Phase Barrier. The solvent dependence of the rotational barrier in DMAAN closely parallels that previously determined for DMA and DMF in aprotic solvents. Figure 2 illustrates the correlation between the barriers in DMAAN and DMA, and it can be seen that with the exception of water and methanol the data cluster around a line with a slope of 1.35. In the absence of a gas-phase measurement, the correlation with DMA has been used to extrapolate an "experimental" value for the gas-phase barrier in DMAAN, based on the known gas-phase barrier for DMA (15.33 kcal/mol).[32] The data points for the protic solvents, water and methanol, were excluded from the fit used for the extrapolation, as was the point for dichloromethane, which appears to be somewhat anomalous.

A very similar gas-phase extrapolation is obtained by plotting the barrier in DMAAN against the Onsager dielectric function, $(\epsilon - 1)/(2\epsilon + 1)$, as shown in Figure 3. For the subset of solvents that are neither hydrogen bonding nor aromatic nor contain second-row elements (methylcyclohexane, dibutyl ether, acetone, acetonitrile, and nitromethane), the data clearly obey a linear relationship. This class of solvents has previously been shown to yield close correlation between rotational barriers in amides and the Onsager dielectric function. The intercept of the best fit line in Figure 3 then yields an estimated gas-phase barrier, since the Onsager dielectric function has a value of zero in the gas phase. The two methods of extrapolation yield as estimates for the gas-phase barrier of DMAAN 9.33 and 9.32 kcal/mol, respectively. The similarity between the extrapolated values is encouraging, as is their very close agreement with the ab initio calculations (QCISD = 9.0 kcal/mol, MP3 = 8.9 kcal/mol, MP2 = 9.9 kcal/mol).

Table 4. Calculated Gas-Phase Basicities and Hydrogen-Bond Affinities of Selected Sites on *N*,*N*-Dimethylacetamide (DMA) and *N*,*N*-Dimethylaminoacrylonitrile (DMAAN)

		gas-phase basicity[a]		
species	site:	C=O/anti[b]	C=O/syn[c]	N
DMA, ES		−217.0	−214.3	−205.0
DMA, TS1		−194.7	−194.1	−218.1
DMA, TS2		−196.0	−201.9	−220.9

		gas-phase basicity[a]	
species	site:	C≡N	amino N
DMAAN, ES		−212.7	−119.7
DMAAN, TS1		−193.8	−210.6
DMAAN, TS2		−194.3	−209.9

[a] HF/6-31+G*, including zero-point energy scaled by 0.8934. [b] Proton or water molecule located anti to nitrogen. [c] Proton or water molecule located syn to nitrogen.

Gas-Phase Proton Affinities. As an aid to understanding the observed solvent effects, gas-phase proton affinities were computed for the equilibrium structure and two possible transition states of DMA and DMAAN, and the results appear in Table 4. The calculations were carried out at the HF/6-31+G* level with zero-point energy corrections scaled by the traditional factor of 0.8934.[33] Due to the lack of consideration of electron correlation, the proton affinities derived from these calculations are likely to show poor absolute accuracy, but for comparisons between DMA and DMAAN they should be adequate. Protonation at both nitrogen atoms of DMAAN was considered, and protonation at nitrogen and both the syn and anti positions of oxygen was considered for DMA. The data show that the equilibrium structure of DMA is 4.3 kcal/mol more basic than the equilibrium structure of DMAAN, and for both species the basicity decreases in the transition state.

Discussion

Charge Reorganization during Bond Rotation. Calculated charge density difference plots have been used in the past to

show the nature and extent of charge redistribution taking place during rotation about conjugated bonds.[34,44] For instance, π-electron density shifts away from the oxygen atom of an amide during C−N bond rotation. This response occurs in the direction predicted by resonance theory, but is of a smaller magnitude than might have been expected. The corresponding charge transfer occurring during bond rotation in thioamides, on the other hand, is considerably greater.[34]

Figure 1 shows that the extent of π-charge transfer away from the nitrile nitrogen atom during bond rotation in DMAAN is so small as to be almost negligible. This observation diverges somewhat from the predictions of a simple resonance picture of the rotational barrier. For comparison, the extent of π-charge transfer at oxygen during bond rotation in formamide is −0.088 electrons; π-charge transfer at sulfur in bond rotation for thioformamide is −0.162 electrons;[34] but π-charge transfer at the nitrile in DMAAN is only −0.016 electrons. Interestingly, the extent of charge redistribution at the vinylic carbon bearing the cyano group is substantially greater (−0.074 π and +0.029 σ), and is comparable to what occurs at the vinylic carbon of vinylamine (−0.089 π and +0.023 σ).[34] DMAAN is perhaps better regarded as a vinylamine substituted with an electron-withdrawing substituent than as a structure akin to a vinylogous amide. Nonetheless, the cyano group substantially increases the rotational barrier, from 5.1 kcal/mol for vinylamine[44] to 7.5 kcal/mol for DMAAN,[45] and so there is clearly an important π-interaction between the cyano group and the amino group.

General Nature of the Solvent Effects. At all levels of calculation, the equilibrium conformer of DMAAN has a larger dipole moment than either of the two transition states. Consequently, a polar medium would be expected to stabilize the equilibrum structure in preference to the transition state, so that the barrier to rotation would increase with solvent polarity. It is readily apparent from Table 3 and Figure 3 that the experimental data support this interpretation. This behavior is analogous to that of DMA and DMF, where the transition states also have lower dipole moments than the minima, and again polar solvents increase the barriers to rotation.[25]

Correlation of Barriers with the Onsager Dielectric Function. Previously it has been shown that the barriers to rotation in DMA and DMF are closely correlated with the Onsager dielectric function, $(\epsilon - 1)/(2\epsilon + 1)$, at least for solvents that are not hydrogen bond donors, are not aromatic, and are not halogenated.[25] Examination of Table 3 and Figure 3 shows that DMAAN follows the same pattern in the solvents methylcyclohexane, dibutyl ether, acetone, acetonitrile, and nitromethane.[46] The lack of correlation for hydrogen bond donating solvents is not surprising, given that any continuum description of the solvent must necessarily neglect the details of hydrogen bonding between solute and solvent. The physical basis for the exclusion of protic solvents is thus clearly defined and well understood.

The reason aromatic and chlorinated solvents deviate from the line is less clear, but at least two possibilities come to mind. First, aromatic π-systems and large second-row atoms such as chlorine are typically characterized by greater electronic polarizability than other organic functional groups. This attribute would lead to stronger than expected short-range interactions with polar solutes, and perhaps as a result to unusually large solvent effects. Alternatively, Newton has shown that carbon tetrachloride engages in unusually strong short-range interactions as a result of its substantial quadrupole moment.[47] These interactions would not be reflected in the bulk dielectric constant, but could certainly influence microscopic solvation behavior. Aromatics are also known to possess substantial quadrupole moments. Consequently the deviation of aromatic and polychloromethyl solvents from the Onsager correlation might reasonably be attributed to electrostatic interactions with the solute that are dominated by the quadrupole moment, rather than the dipole moment, of the solvent species.

The Absence of a Hydrogen-Bonding Effect. A very interesting feature of the DMAAN system is that solvent hydrogen bond donor ability appears to have no effect on the barrier to C−N bond rotation, or perhaps even a modest negative effect. This observation contrasts strikingly with the behavior of DMA and DMF, which both show significantly higher barriers in protic solvents than in aprotic solvents of comparable polarity.[48] Thus, for instance, methanol and water fall on the same line in Figure 3 as do the other solvents. Furthermore, as the experimental value for water only represents an upper limit, the barrier might actually be lower in water than it is in methanol. With DMA and DMF, on the other hand, methanol and water increase the barriers to rotation by 1.0−1.5 kcal/mol relative to polar aprotic solvents such as acetone, and the barriers are significantly higher in water than in methanol.[25,49] This difference in behavior between protic and aprotic solvents of comparable polarity[48] has been attributed to solvent hydrogen bond donation to the carbonyl oxygen, which is more favorable in the equilibrium structure than in the transition state.[25,30] Apparently, this effect is absent in DMAAN.

The discrepancy is also evident in Figure 2, which compares the barriers of DMA and DMAAN in a variety of solvents. The barriers are related in a highly linear fashion, except for the cases of water and methanol, for which the solvent effects diverge. The same point is illustrated in Figure 4a, where it can be seen that the solvent effects on DMAAN correlate in a very linear fashion with the empirical solvent polarity parameter *S* for all solvents explored except water and methanol, for which there are again significant deviations from the line. Previously reported data for the solvent effects on C−N bond rotation in DMF and DMA also correlate closely with this parameter, as shown in Figure 4b, but for the amides, water and methanol do not deviate from the pattern of other solvents.

What is the reason for the lack of a contribution from hydrogen bond donor ability to the rotational barrier of DMAAN? There are in principle three possibilities: (1) There is no significant hydrogen-bonding contribution to the solvation of DMAAN in either the equilibrium structure or the transition state structure. (2) Hydrogen bonding to DMAAN takes place, but the nature and strength of the hydrogen bonding does not significantly change on going from the minimum to the transition state. (3) There are significant changes in hydrogen bonding between the minimum and the transition state of

(44) Wiberg, K. B.; Rablen, P. R. *J. Am. Chem. Soc.* **1993**, *115*, 9234−9242.

(45) The values given here (5.1 kcal/mol for vinylamine, 7.5 kcal/mol for DMAAN) are calculated enthalpies at 0 K.

(46) It is worthy of note that the data point for acetonitrile in Figure 3 lies somewhat above the best fit line, indicating a higher barrier than in other solvents having comparable values for the Onsager dielectric function. This deviation possibly indicates that acetonitrile, like the aromatic and chlorinated solvents, yields somewhat stronger than expected interactions with polar solutes due to unusually great electronic polarizability. The "soft" π-system of acetonitrile could certainly account for such polarizability. A similar pattern was observed with DMA and DMF previously, where again acetonitrile yielded a somewhat stronger solvent effect than did acetone.

(47) (a) Perng, B.-C.; Newton, M. D.; Raineri, F. O.; Friedman, H. L. *J. Chem. Phys.* **1996**, *104*, 7153−7176. (b) Perng, B.-C.; Newton, M. D.; Raineri, F. O.; Friedman, H. L. *J. Chem. Phys.* **1996**, *104*, 7177−7204.

(48) "Polarity" here is meant as measured by the Onsager dielectric function.

(49) Rablen, P. R. Ph.D. Thesis, Yale University, 1994.

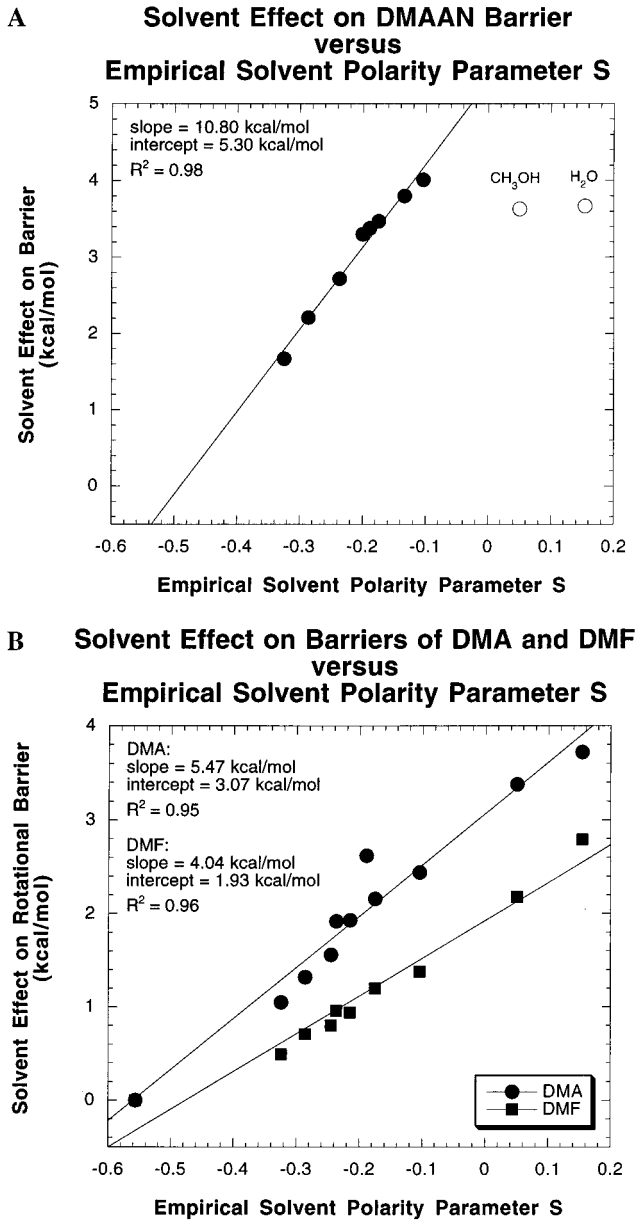

Figure 4. (a) Relationship between the experimental solvent effect on the barrier to C−N bond rotation in DMAAN and the empirical solvent polarity parameter *S*. Best fit line: barrier (kcal/mol) = 10.80∗*S* + 5.30; r^2 = 0.98. The data points represented by open circles were excluded from the fit. (b) Relationship between the experimental solvent effect on the barrier to C−N bond rotation in DMA and DMF and the empirical solvent polarity parameter *S*. Best fit lines: DMA barrier (kcal/mol) = 5.47∗*S* + 3.07; r^2 = 0.95; DMF barrier (kcal/mol) = 4.04∗*S* + 1.93; r^2 = 0.96.

DMAAN, but the changes are complex and result in little net change in energy. For instance, changes in hydrogen bonding at the amino nitrogen could in principle counterbalance any changes at the cyano nitrogen. One variation of this last possibility is that some hydrogen bonding to the amino nitrogen occurs even in the equilibrium structure, and catalyzes the bond rotation process, thus counteracting any retarding effect resulting from hydrogen bonding at the nitrile. It is known that Lewis acids can catalyze bond rotation about amides in exactly this manner.[3] These possibilities are explored in detail in the paper following this one via further ab initio calculations and statistical mechanical simulations.

Even at a fairly qualitative level, however, it is not surprising that hydrogen bonding plays a comparatively smaller role in the solvation of DMAAN than in that of DMA. DMAAN has a larger dipole moment than DMA, and so ordinary solvent polarity has a stronger influence on DMAAN than on DMA. This difference is reflected in the larger solvent effects predicted and observed for DMAAN relative to those in DMA. On the other hand, the calculated proton affinities appearing in Table 4 demonstrate that DMAAN is less basic than DMA. The lower basicity might be expected to translate into weaker hydrogen-bonding interactions with solvent molecules, and consequently to a smaller solvent effect enhancement from protic solvents. Furthermore, Figure 1 demonstrates that bond rotation has very little effect on the electron density distribution at the primary hydrogen-bonding site, the nitrile nitrogen atom. That in turn suggests that changes in the solvation energy occurring during bond rotation will be dominated by bulk dielectric response rather than by specific short-range interactions such as hydrogen bonds. Nonetheless, the complete absence of an apparent hydrogen-bonding term is somewhat surprising.

Correlation of the Barriers with Empirical Solvent Polarity Scales. Empirical solvent polarity scales abound,[8] and it might be expected that some of these scales would yield good correlations with the experimental data for DMAAN. It has previously been shown that the solvent effects on DMA correlate quite closely with the spectroscopic solvent polarity parameter E_t.[25,50] Figure 4b shows that such a correlation also exists for both DMF and DMA with Brownstein's parameter *S*, which is a composite measure of solvent polarity derived from a series of spectroscopic determinations.[8,51] Figure 4a demonstrates that the data for DMAAN also correlate closely with *S*. The data are likely to correlate well with a wide variety of other empirical solvent polarity scales as well, and the analysis provided here is meant to be representative rather than comprehensive.

The close correlation of the data for DMA, DMF, and DMAAN with *S* suggests that this parameter captures the essence of how most solvents affect bond rotation processes in polar conjugated molecules such as amides. Perhaps this correlation is not surprising. When electronic excitation occurs, changes in solute structure occur very rapidly, so that the initial condition of solvation of the excited state is not equilibrated. Although rotation about the conjugated C−N bond of DMA, DMF, or DMAAN is in some sense a slow process, the actual molecular motions involved are very rapid. Although these nuclear motions are not nearly as rapid as electronic excitation, they nonetheless occur on a time scale comparable to that for the reorientation of solvent molecules. Thus one cannot assume that solvent reorganization is greatly *faster* than the conformational change, as would be necessary for a separation of time scales argument. Consequently, the transition state quite likely does not achieve fully equilibrated solvation. Perhaps *S* describes changes in solvation between an equilibrium structure and a fleeting transition state structure more accurately than does a purely equilibrium property such as the dielectric function. Stated another way, since *S* is defined in terms of an extremely rapid process (absorption of light), it is probably well-suited to describing solvent effects on other transformations that involve molecular motions at least as rapid as solvent reorganization.

The value of *S* is defined for the gas phase, and thus Figure 4a allows an additional method for extrapolating the gas-phase barrier to rotation in DMAAN from the available experimental

(50) (a) Kosower, E. M. *J. Am. Chem. Soc.* **1958**, *80*, 3253−3260. (b) Kosower, E. M.; Mohammad, M. *J. Am. Chem. Soc.* **1968**, *90*, 3271−3272. (c) Kosower, E. M.; Mohammad, M. *J. Am. Chem. Soc.* **1971**, *93*, 2713−2719. (d) Mohammad, M.; Kosower, E. M. *J. Phys. Chem.* **1970**, *74*, 1153−1154.

(51) Brownstein, S. *Can. J. Chem.* **1960**, *38*, 1590.

solution data. Using the best fit line shown in Figure 4a yields an estimate of 8.6 kcal/mol for the gas-phase barrier. This value is somewhat lower than that obtained by the previously described extrapolations (9.3 kcal/mol), but is still in the same vicinity and in close agreement with the ab initio calculations. None of the qualitative conclusions in this paper would change as a result of using this alternative estimate for the gas-phase barrier, and the quantitative conclusions would only change modestly.

Summary

The barrier to rotation about the conjugated C−N bond in DMAAN has been determined by dynamic NMR spectroscopy in a wide variety of solvents and at a series of temperatures. In analogy to the case of amides, the barrier increases with the polarity of the solvent. Qualitative electrostatic arguments can account for this behavior, by pointing out that the equilibrium structures of these species have larger dipole moments than the corresponding transition states for C−N bond rotation. The variation of the DMAAN barrier with solvent closely parallels the pattern observed previously for DMA, such that a plot of the one barrier versus the other as a function of solvent yields a close fit to a straight line as long as protic solvents are excluded. The data also follow a linear relationship with respect to Brownstein's empirical polarity parameter *S*. Although the barrier for DMAAN in the gas phase was not determined experimentally, the linear relationship of the available solution data with the corresponding data for DMA allows the extrapolation of a gas-phase estimate, 9.3 kcal/mol, that agrees closely with the results of high-level (MP2, MP3, and QCISD) ab initio calculations. For aprotic, nonaromatic solvents lacking chlorine atoms, the barriers are linearly related to the Onsager dielectric function, $(\epsilon - 1)/(2\epsilon + 1)$. This correlation yields an estimated gas-phase barrier that agrees very closely with those obtained from the other empirical relationships.

In stark contrast to the case of amides, however, protic solvents do not cause a further increase in the barrier for DMAAN above that observed in other polar solvents. While the barrier heights in DMAAN are for the most part linearly related to both *S* and the barriers observed for DMA, the data points for the protic solvents methanol and water diverge strongly from these lines. It is postulated that much weaker or less prevalent hydrogen bonding to the nitrile of DMAAN, as compared to the carbonyl of amides, is at least partly the cause of this difference. Some support for this notion is provided by the calculated proton affinities of DMAAN and DMA, which show DMAAN to be significantly less basic than DMA, and also by a calculated difference density plot, which shows that little electronic reorganization occurs at the cyano nitrogen during the bond rotation process.

Experimental Section

Sample Preparation. DMAAN was obtained from Aldrich and distilled under vacuum prior to use. Deuterated solvents were obtained from Cambridge Isotope Laboratories (butyl ether-d_{18}) or Aldrich (all other cases). NMR samples were prepared by placing 2 mL of DMAAN in approximately 0.8 mL of the appropriate solvent in an NMR tube. The solution was then subjected to five cycles of freeze−pump−thaw, with cooling in liquid nitrogen, dry ice/acetone, or ice water, to accomplish degassing. The degassed and evacuated sample was then flame-sealed. In the case of dibutyl ether and methylcyclohexane, lower concentrations of sample were used: for methylcyclohexane, 0.5 mL of DMAAN were placed in 0.8 mL of solvent, and for dibutyl ether, 1.0 mL of DMAAN was placed in 0.8 mL of solvent.

Calibration of a Variable-Temperature NMR Probe. All NMR experiments were carried out on a Brüker AM-400 (400 MHz) spectrometer operated by an Indy workstation and equipped with a variable-temperature 5-mm probe. The calibration of the probe's temperature controller was established at least once per week against a vacuum-sealed methanol standard, or else immediately before or immediately after a given rate-measurement experiment. Actual probe temperature was determined from the equation below, in which $\Delta\delta$ is the chemical shift difference in ppm between the two peaks in the neat methanol sample.[52]

$$T(K) = 409.0 - 36.54(\Delta\delta) - 21.85(\Delta\delta)^2$$

In general, the calibrated temperature corresponding to a given temperature setting did not vary by more than ±0.5° from one week to the next. Variability was even lower for temperatures near room temperature, but occasionally somewhat greater (∼±1.0°) for temperatures far above or below room temperature.

Line Shape Fitting Experiments. An ordinary one-dimensional NMR spectrum was taken with a 30° pulse, a 10 s predelay, a spectral width of 2000 Hz, an offset of 3.0 ppm, a 16K data block, and from 32 to 256 scans. No line broadening was added. The spectra were then transformed into ASCII form by using the tojdx command, and the appropriate portion of the spectrum was extracted by using a FORTRAN conversion program CVT_NMR.[53]

Fitting to the experimental spectrum was then accomplished using another FORTRAN program, MUTEX,[54] which implements the equations shown below. These equations, taken from Sandström,[38] describe the signal shape from a pair of uncoupled but mutually exchanging resonances.

$$v = -C_0 \frac{\left\{P\left[1 + \tau\left(\frac{p_B}{T_{2A}} + \frac{p_A}{T_{2B}}\right)\right] + QR\right\}}{P^2 + R^2}$$

where

$$\delta\nu = \nu_A - \nu_B \qquad \Delta\nu = {}^1/_2(\nu_A - \nu_B) - \nu \qquad \tau = \frac{p_A}{k_B} = \frac{p_B}{k_A}$$

$$P = \tau\left[\frac{1}{T_{2A}T_{2B}} - 4\pi^2\Delta\nu^2 + \pi^2\delta\nu^2\right] + \frac{p_A}{T_{2A}} + \frac{p_B}{T_{2B}}$$

$$Q = \tau[2\pi\Delta\nu - \pi\delta\nu(p_A - p_B)]$$

$$R = 2\pi\Delta\nu\left[1 + \tau\left(\frac{1}{T_{2A}} + \frac{1}{T_{2B}}\right)\right] + \pi\delta\nu\tau\left(\frac{1}{T_{2B}} - \frac{1}{T_{2A}}\right) + \pi\delta\nu(p_A - p_B)$$

In these equations, the parameters p_A and p_B refer to the populations of the two exchanging sites, ν_A and ν_B refer to the intrinsic chemical shifts, T_{2A} and T_{2B} give the effective relaxation times for the separate peaks (i.e., the intrinsic line widths), and k_A is the rate constant for exchange. Rate constants were obtained by minimizing the difference between the calculated and experimental spectra. Line shape fitting suffers from the need to establish the natural line width by some independent means to obtain reliable rate constants. This determination was accomplished by using the TMS line to measure the "intrinsic" line width (quality of shimming) under each set of experimental conditions. It was found that in the regime of extremely slow exchange, the DMAAN methyl peaks and the TMS peak reliably showed the same line width.

Selective Inversion−Recovery Experiments. Selective inversion−recovery (SIR) experiments were carried out in the standard fashion.[40−42] The standard SIR pulse sequence shown below was used, where t_{ev} is the evolution time and t_{mix} is the mixing time.

(52) Ammann, C.; Meier, P.; Merbach, A. E. *J. Magn. Reson.* **1982**, *46*, 319−321.
(53) Rablen, P. R. *CVT_NMR*, Swarthmore College, 1996.
(54) Rablen, P. R. *MUTEX*, Yale University, 1993.

$$90°_x \rightarrow t_{ev} \rightarrow 90°_y \rightarrow t_{mix} \rightarrow 90°_x \rightarrow \text{observe (FID)}$$

The offset frequency was set to exactly halfway between the two exchanging methyl peaks, and the evolution time was set to one-half the reciprocal of the difference in the two peak positions in hertz. The mixing time was assigned a series of values corresponding to roughly 5 half-lives for the exchange process. Typically, 10−15 different mixing times were used for each rate measurement, and 4 scans were taken for each spectrum. A delay between pulses of 130 s was used to avoid artifacts from incomplete relaxation. The data block size was always set to 16K, the spectral width set to 2000 Hz, the pulse width calibrated to 90°.

The integrated peak intensities for a given series of mixing times were then fit to the equation below in a least-squares sense.[55]

$$\ln\left(\frac{(M_0 - M_{za}(t)) - (M_0 - M_{zx}(t))}{(M_0 - M_{za}(t)) + (M_0 - M_{zx}(t))}\right) = -2k_r t$$

M_0 refers to the equilibrium magnetization (intensity), $M_{za}(t)$ the magnetization of peak A at mixing time t, $M_{zx}(t)$ the magnetization of peak X at mixing time t, and k_r the rate constant for exchange. The fitting was accomplished using a FORTRAN program.[56] These equations assume equal t_1 relaxation times for the two methyl peaks, and make some other assumptions as well. However, as long as exchange is fairly rapid compared to longitudinal relaxation, whether this assumption is correct makes almost no difference for the computed rate constant. Perrin has used a much more sophisticated equation, having seven adjustable parameters and making fewer assumptions, to model his SIR data.[43] However, we have chosen the simple equations above in the hopes that, with only two adjustable parameters, any serious problems with the data would reveal themselves as a nonlinear plot. In actual fact, an extremely high degree of linearity was obtained, with r^2 values typically 0.99 or better, and almost never below 0.98, although in some cases with slow exchange only 2 or 3 half-lives could be used.

Ab Initio Calculations. The Gaussian 94 package[57] was used to carry out all ab initio calculations. Standard Pople-type basis sets were used,[58] with six Cartesian d functions in all cases. The nature of all stationary points was verified by calculation of the HF/6-31G* vibrational frequencies. Density = current was specified for MP2 calculations to ensure use of the correlated charge density distribution for determination of molecular dipole moments.

The methodology for obtaining and integrating the difference density appearing in Figure 1 has been described in detail elsewhere.[34,44] Briefly, an MP2/6-31G* optimization was performed to obtain a partially equilibrated structure in which the HC═CHCN fragment was frozen at the transition state (TS #2) geometry, i.e., only the dimethylamino group was allowed to move. Single-point calculations were then carried out at the MP2/6-311++G** level at this modified "equilibrium" geometry and also at the transition state geometry. Subtraction of the charge density distribution for the latter from that for the former then provided the desired difference density, represented numerically as a cubic grid 20 Bohr in length along each axis and with points spaced 0.20 Bohr apart. Restriction of geometric freedom is required to avoid artifacts arising from slight movement of atoms in the immediate vicinity of interest (the HC═CHCN fragment). The geometric constraints in this case raised the energy by 2.7 kcal/mol, which is relatively small compared to the rotational barrier, and so the difference density shown should have at least semiquantitative meaning. In Figure 1, regions of the difference density associated with movement of the methyl groups have been removed to allow easier visualization.

Integration of the charge density was performed for each separate region visible in Figure 1 by summing the contributions from all points for which the difference density remained higher than a specified contour. This procedure was then carried out for a series of contour definitions to facilitate an extrapolation of the results to a hypothetical zero contour. This methodology has been described in detail previously.[34,44]

Acknowledgment. Financial support for this work was provided by a Faculty Start-up Grant for Undergraduate Institutions from the Camille and Henry Dreyfus Foundation, by a Cottrell College Science Award of Research Corporation, and by Swarthmore College. Acknowledgment is also made to the donors of the Petroleum Research Fund, administered by the American Chemical Society, for partial support of this research. We thank Kenneth Wiberg of Yale University for helpful discussions and preliminary review of the manuscript.

Supporting Information Available: Ab initio calculated energies in Hartrees, calculated molecular geometries in *Z*-matrix form, and complete tabulation of experimental rate constants (PDF). See any current masthead page for Web access instructions.

JA982304F

(55) Harris, R. K. *Nuclear Magnetic Resonance Spectroscopy*; John Wiley & Sons: New York, 1987; p 172.

(56) Rablen, P. R. *SIR*; Yale University, 1994.

(57) Frisch, M. J.; Trucks, G. W.; Schlegel, H. B.; Gill, P. M. W.; Johnson, B. G.; Robb, M. A.; Cheeseman, J. R.; Keith, T.; Petersson, G. A.; Montgomery, J. A.; Raghavachari, K.; Al-Laham, M. A.; Zakrzewski, V. G.; Ortiz, J. V.; Foresman, J. B.; Cioslowski, J.; Stefanov, B. B.; Nanayakkara, A.; Challacombe, M.; Peng, C. Y.; Ayala, P. Y.; Chen, W.; Wong, M. W.; Andres, J. L.; Replogle, E. S.; Gomperts, R.; Gonzalez, C.; Martin, R. L.; Fox, D. J.; Binkley, J. S.; Defrees, D. J.; Baker, J.; Stewart, J. P.; Head-Gordon, M.; Gonzalez, C.; Pople, J. A. *Gaussian 94* (Revision C.2); Gaussian, Inc.: Pittsburgh, PA, 1995.

(58) Hehre, W. J.; Radom, L.; Schleyer, P. v. R.; Pople, J. A. *Ab Initio Molecular Orbital Theory*; Wiley: New York, 1986.